REPORT DOCUMENTATION PAGE

AFRL-SR-AR-TR-02-

0454

1. AGENCY USE ONLY (Leave blank)	2. REPORT DATE	3. REPORT TYPE AND DATES COVERED
	November 15, 2002	Final Report 10/1/98-3/31/02

4. TITLE AND SUBTITLE
Control of Sound Radiation and Reflection with Advanced Smart Acoustic Blankets

5. FUNDING NUMBERS
F49620-99-1-0020

6. AUTHOR(S)
Dr. Chris R. Fuller

7. PERFORMING ORGANIZATION NAME(S) AND ADDRESS(ES)

Virginia Polytechnic Institute & State University
460 Turner Street, Suite 306
Blacksburg, VA 24060

8. PERFORMING ORGANIZATION REPORT NUMBER
4-30778

9. SPONSORING / MONITORING AGENCY NAME(S) AND ADDRESS(ES)

Dean Mook, Technical Monitor
Air Force Office of Scientific Research
801 N. Randolph Street, MS 732
Arlington, VA 22203-1977

10. SPONSORING / MONITORING AGENCY REPORT NUMBER

11. SUPPLEMENTARY NOTES

12a. DISTRIBUTION / AVAILABILITY STATEMENT

Approved for public release; distribution unlimited.

12b. DISTRIBUTION CODE

13. ABSTRACT *(Maximum 200 Words)*

The work carried out in this project has successfully demonstrated the potential of advanced smart acoustic blankets for reducing sound transmitted into payload fairings. The smart blanket consists of active tiles embedded in standard acoustic blanket material. The lightweight honeycomb tiles are supported by specially developed active-passive piezoelectric mounts, which implement Thunder elements. The mounts are designed to provide passive isolation of transmitted sound, which is augmented by the application of active inputs in parallel to the mount. SISO uncoupled control approaches were developed in order to facilitate the future use of multiple active tiles. Both feedforward and feedback control approaches applied to a single tile located on a payload fairing like structure provided good reduction of broadband transmitted sound. The feedback approach is especially attractive due to its low complexity and cost effectiveness of hardware. An analytical model of the active tile system applied to a base structure has been developed and used to optimally design the system.

14. SUBJECT TERMS			15. NUMBER OF PAGES 23
			16. PRICE CODE
17. SECURITY CLASSIFICATION OF REPORT	18. SECURITY CLASSIFICATION OF THIS PAGE	19. SECURITY CLASSIFICATION OF ABSTRACT	20. LIMITATION OF ABSTRACT

Final Performance Report

On

AFOSR Grant No: F49620-99-1-0020

CONTROL OF SOUND RADIATION AND REFLECTION WITH ADVANCED SMART ACOUSTIC BLANKETS

By

Prof. Chris R. Fuller, PI

Vibration and Acoustics Laboratories
Mechanical Engineering Department
Virginia Tech
Blacksburg, VA 24061
Email: c.r.fuller@larc.nasa.gov

November, 2002

1. OBJECTIVES

This report summarizes theoretical and experimental work on developing smart acoustic blankets for increased transmission loss of sound into AF launch vehicle payload fairings under AFOSR Grant No: F49620-99-1-0020. The investigation concentrates at the low frequencies (below 250Hz) where the conventional passive blankets have proved to be ineffective [1]. The approach investigated at VAL consists of a hybrid active-passive approach in which active elements are combined with the conventional passive blanket treatment to improve its low frequency performance. The physical basis of the smart acoustic blanket is also based upon the smart skin approach under development at VAL for the last five years [2,3,4]. A smart skin is designed to cover the complete structure or extended regions of the structure through which most of the acoustic power transmits. It functions by reducing the radiation impedance that the structure sees (effectively de-couples the structural motion from the acoustic field) without having to apply control forces directly to the structure itself [4]. The smart skin approach is thus very suitable for very stiff structures such as a typical payload fairing.

The following report will summarize progress in investigating, developing and implementing a candidate smart skin. Practical aspects of the approach will also be summarized followed by some suggestions for future work.

2. STATUS OF EFFORT

The work carried out in this project has successfully demonstrated the potential of advanced smart acoustic blankets for reducing sound transmitted into payload fairings. The smart blanket consists of active tiles embedded in standard acoustic blanket material. The lightweight honeycomb tiles are supported by specially developed active-passive piezoelectric mounts, which implement Thunder elements. The mounts are designed to provide passive isolation of transmitted sound, which is augmented by the application of active inputs in parallel to the mount. SISO uncoupled control approaches were developed in order to facilitate the future use of multiple active tiles. Both feedforward and feedback control approaches applied to a single tile located on a payload fairing like structure provided good reduction of broadband transmitted sound. The feedback approach is especially attractive due to its low complexity and cost effectiveness of hardware. An analytical model of the active tile system applied to a base structure has been developed and used to optimally design the system.

3. ACCOMPLISHMENTS/NEW FINDINGS

3.1 Preliminary Investigations

Preliminary work in the project investigated various smart blanket concepts. These concepts were evaluated for potential before the final design, which is discussed in detail below, was chosen. We briefly summarize the preliminary work on alternative concepts.

The first concept was based around constructing a smart blanket from acoustic foam with embedded active elements of the piezo polymer PVDF as shown in Figure 1. The smart blanket consists of a composite construction of foam and honeycomb sheet. Active elements are located on the honeycomb sheet and/or embedded in the foam.

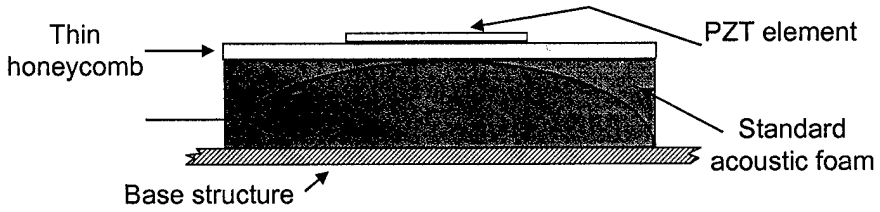

Figure 1. Composite smart blanket

A Finite Element model of the smart foam elements with embedded curved PVDF piezoelectric layers was developed and tested. The numerical model was also extended to model the behavior of the experimental rig described below. The numerical model was exercised to investigate and understand the physics of the smart acoustic foam as well as optimally design smart foam elements for the test rig.

A 1D experimental rig was constructed for l testing of the smart foam elements. The rig consisted of a long hard walled tube excited by a speaker at one end and anechoically terminated (i.e. no reflections) at the other as shown in Figure 2. Smart foam test samples were located in the center of the tube. Typical samples are presented in Figure 3.

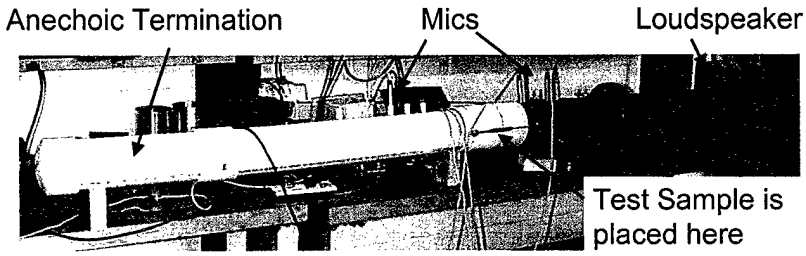

Figure 2. Blanket test rig for normal incidence sound field.

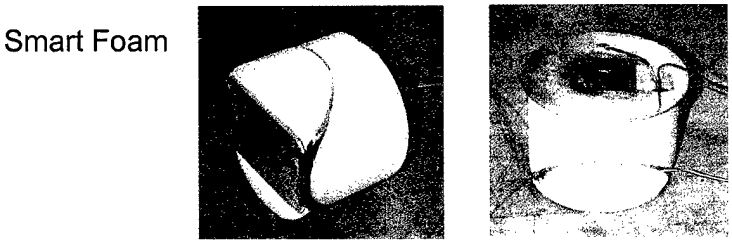

Figure 3. Typical smart blanket samples.

The incident acoustic wave amplitude was measured in the upstream section using a two microphone technique while a single microphone was located down stream of the test section. These measurements enabled evaluation of the acoustic power transmission loss (TL) of various smart foam test samples under normal acoustic incidence. A schematic of the test set up in instrumentation is given in Figure 4

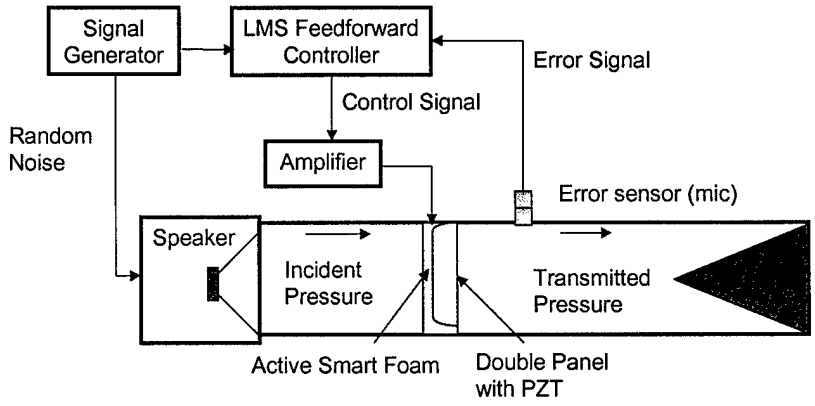

Figure 4. Schematic of test set up and instrumentation

Two different electronic damping circuits were constructed and tested. The first was a conventional RL circuit designed to resonate at the test frequency. The second circuit involved the use of a negative capacitance to cancel the capacitance of the piezoelectric element and use a resistance to dissipate electrical energy. These circuits were implemented on a circuit breadboard and used solid state inductances.

Various configurations of smart foam elements were constructed and tested in the TL rig in conjunction with the electronic "damping" circuits discussed above. The main configurations tested were; (1) acoustic foam with single and multiple layers of embedded PVDF. (2) acoustic foam with PVDF glued to the surface. (3) acoustic foam with a thin metal layer glued to the surface of the foam. A small piezoceramic element was glued to the metal plate and (4) the same as configuration 2. except that the plate was not glued to the foam but instead a small air gap was left. The two electronic circuits described above were tested. The main results obtained are summarized as follows.

Configuration (3) gave over 10dB increase in TL when the standard "damping" circuit was implemented. This occurred at the circuit design resonance whether the plate-smart foam system was on resonance or not. This implied that the RL circuit does not actually "damp" energy in the resistor but actually is an electrical equivalent of tuned vibration absorber. The RL circuit in conjunction with the piezoelectric device thus reduced sound transmission by applying a strain to the plate and stiffening it. This was confirmed by removing the resistance and obtaining the same attenuation (i.e. electrical energy is not dissipated in the resistance). This is very useful as it implies this type of configuration can operate off the structural system resonance and at multiple frequencies. When the negative capacitance circuit was tested with configuration (3) the TL was only increased by 2dB and at only the plate foam system structural resonance. The low attenuation was though to be due to not accurately measuring the PZT impedance (or capacitance) and new tests will be carried out with an impedance meter to improve this. The fact that attenuation occurs only at the structural system resonance also implies that the negative capacitance circuit acts by real electrical damping or dissipation in the load resistance. These aspects were investigated in detail using the smart foam FE model in conjunction with electrical circuit models. Configuration (4) gave similar results to (3) confirming that the attenuation of the plate vibration was not due to the physical contact of the acoustic foam.

Tests on configurations (1) and (2) were inconclusive. A FRF of the PVDF output showed a resonance peak corresponding to the smart foam element dimensions. Tests using the conventional electrical circuit gave no appreciable increase in TL and this can be understood from the above discussions. If this circuit functions by reactive effects as believed then the PVDF will not be able to "stiffen" the foam globally. Tests with the negative capacitance circuit gave negligible improvements in TL (of the order of 1 to 2db) and this was thought to be due to mistuning of the circuit and design and layout of the PDFV elements to extract maximum vibration energy from the foam.

Figures 5 and Figure 6 show example results. In Figure 5 the blanket system consisted on foam covered on one or both sides with honeycomb sheet and embedded PVDF in the foam. A feedforward approach is used to actively minimize the transmitted sound waves. The results show quite impressive broadband performance. In Figure 6 a similar system is tested except that the active input is a PZT actuator located on the downstream honeycomb covering sheet. The results are gain impressive.

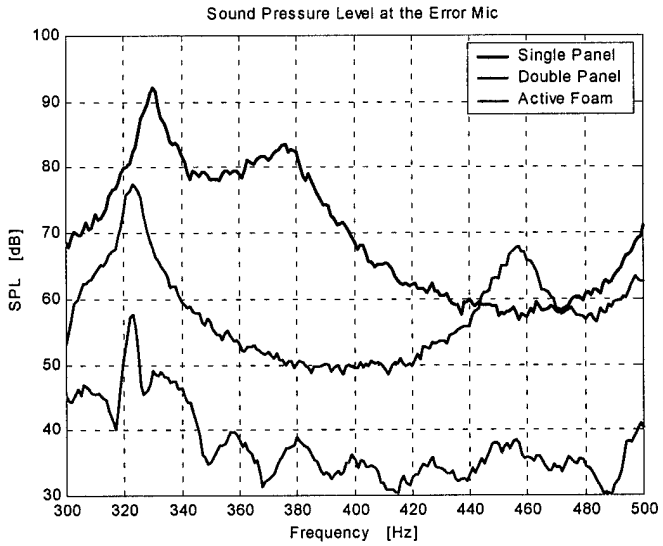

Figure 5. Smart foam blanket test results.

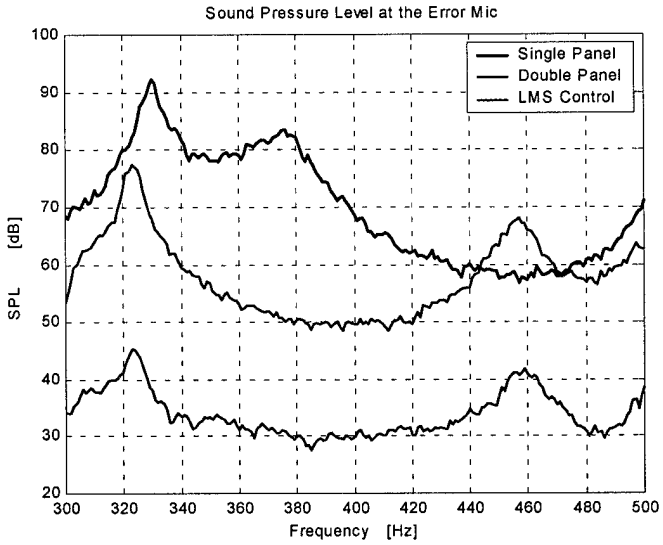

Figure 6. Active panel blanket test results.

Transmission loss tests using such a system were also performed in the TL facility at VT. Figure 7 is a photograph of the concept extended from a 1D system to a 2D panel system. Evident in the photographs are the honeycomb top covering plates and the active PVDF and PZT piezoelectric elements. TL tests with the system provided reasonable broadband control similar to that shown in Figures 5 and 6. However this approach was discontinued for the reasons discussed next.

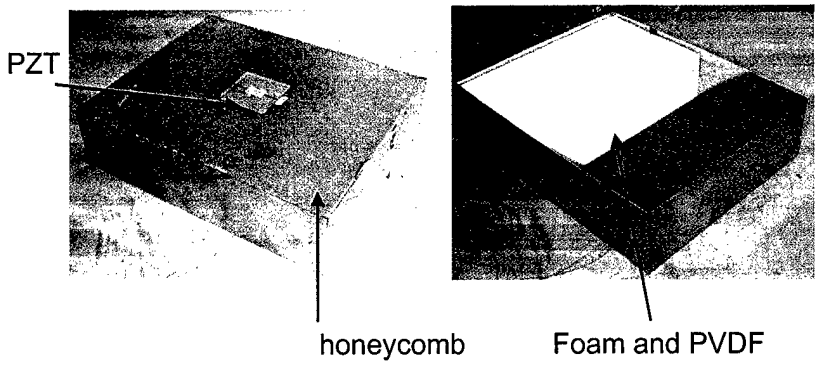

Figure 7. 2D smart blanket construction.

Tests were also performed to check the maximum level of the incident wave that could be controlled by the embedded PVDF. This was found to be limited by the maximum drive level of the PVDF and PZT piezoelectric elements. Typical maximum sound pressure levels that could be controlled were approximately 100-110dB at 150 Hz. While this is significant it is still much less than incident levels that would be encountered in realistic payload applications. Alternative arrangements thus need to be investigated and these are discussed in Section 1.3.

Another approach that was studied was the concept of a subsonic skin. It is well known that the sound radiation occurs only from supersonic wave motion on the vibrating structure. Thus if the structure is covered with a skin that transforms the supersonic wave motion into subsonic then the sound radiation will be vastly reduced. Figure 8 shows a schematic of such a concept.

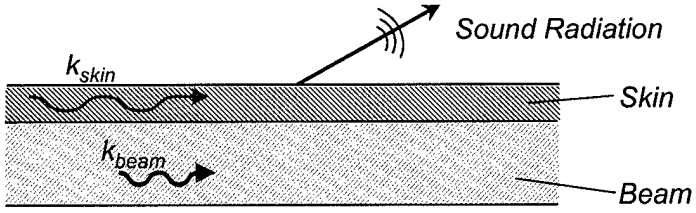

Figure 8. Subsonic skin concept.

The approach followed was based upon coupled waveguides. If a skin (or wave guide) can be constructed so as to only support subsonic motion then it could be used to cover the offending sound radiating structure. Energy will then leak from the supersonic waves on the base structure (the fairing) into the subsonic motion via the coupling interface and thus sound radiation should fall. To investigate the potential of this concept an analytical model was constructed. The model is shown in Figure 9 and consists of a series of coupled SDOF mass spring elements. Wave motion in the mass spring elements occurs due to the spring that laterally couples them. A piston is located on the top of each element to create sound radiation. The parameters of the mass spring skin can be adjusted to ensure that the wave speed is subsonic in the frequency range of interest.

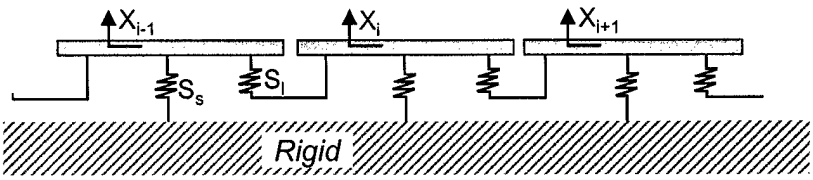

Figure 9. Model of subsonic skin.

A mathematical model of the subsonic skin was developed and used to study the behavior of the skin attached to a beam. Example results are shown in Figures 10 and 11. Both figures results of spatial and frequency Fourier transforms of the skin normal displacement versus frequency (a dispersion plot) obtained from the model beam excited by an impulse. Also shown is the acoustic wavenumber as a dark straight line. Figure 10 gives results for a generic layer and the layer is clearly supersonic (wavenumber for the layer greater than the acoustic wavenumber) over all its frequency range. Figure 11 presents results for a tuned layer where the parameters are chosen to ensure that the layer wave is subsonic. It can be seen that indeed the layer wave is slower than the acoustic wave.

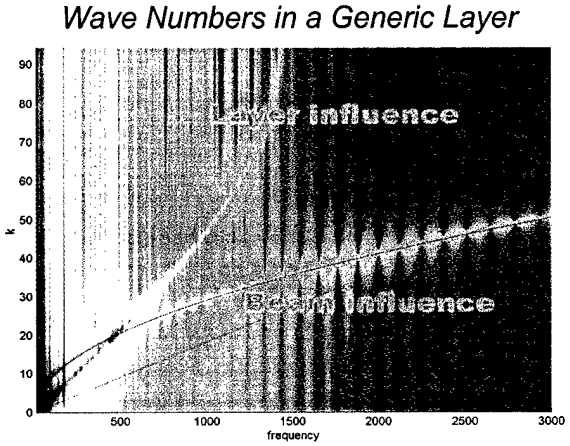

Figure 10. Dispersion plot for a generic skin.

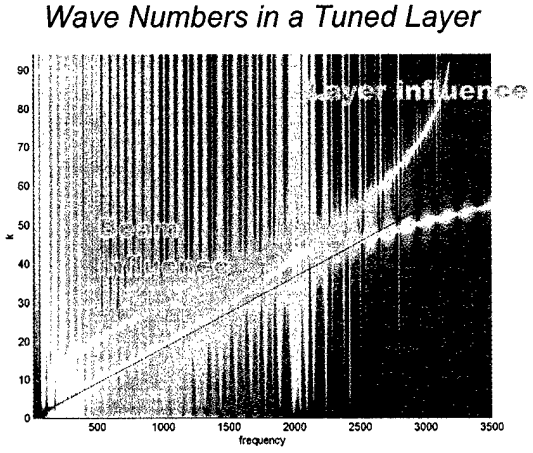

Figure 11. Dispersion plot for a tuned skin.

While these results showed promise for designing advanced smart blankets for payload noise reduction it was felt that the implementation would not be practical in 2D and very difficult to construct.

Main conclusions of the preliminary investigations.

1. The conventional RL circuit acts by reactive effects not damping as previously believed by other researchers. This circuit is thus useful for electronic damping on distributed elastic systems such as plates etc but not foam systems.
2. A plate-smart foam system gave an increase in sound transmission loss of 10dB with a conventional damping circuit.

3. The foam-PVDF composites rely on extracting energy by electronic damping thus the electrical circuit must perform this function. The negative capacitance circuit shows potential for this but the capacitance of the PVDF must be measured accurately.
4. The smart foam elements have demonstrated potential for efficiently (i.e. light weight, low power etc) increasing sound transmission loss of structures.
5. However the smart foam elements do not appear to have sufficient control authority for payload fairing noise control applications.
6. A Finite Element model of the smart foam elements has been developed and proved useful for investigating system behavior and optimal design.
7. The subsonic skin showed potential for reducing sound transmission. However construction in a 2D arrangement would be extremely difficult.

3.2 Design concept

The preliminary work discussed above showed potential but its practicality was limited by various aspects and the approaches were discontinued. In order to develop a viable solution a new concept was derived based upon the systems and knowledge gained in the preliminary investigations. We now discuss this system, which ultimately proved satisfactory.

Figure 12 shows a schematic of the smart skin positioned over a section of the payload fairing structure. The smart skin consists of active tiles embedded in acoustic foam (not shown for clarity). The acoustic foam provides the high frequency passive attenuation while the active tiles provide the low frequency active control of the transmitted sound. Figure 13 shows a schematic of an individual tile element. The tile element consists of a lightweight, very stiff panel connected to the payload fairing base structure by active actuators that consist of a spring-damper with an active force applied in parallel to each mount. Acoustic foam is located underneath and on top of the tile in order to control high frequency sound transmission and increase cavity absorption respectively.

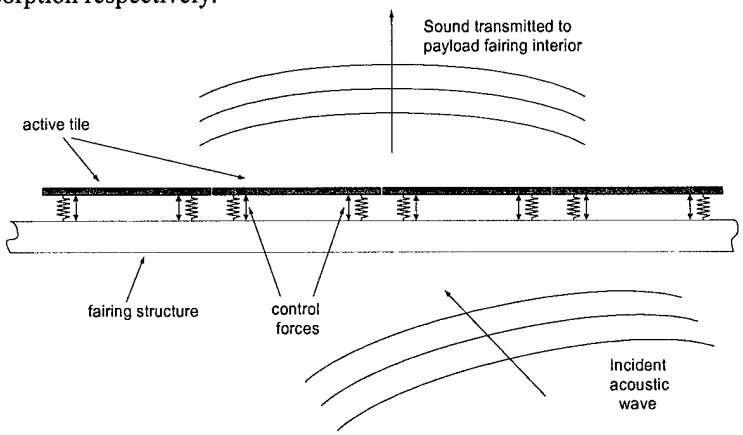

Figure 12. Generic smart skin for plf sound transmission control.

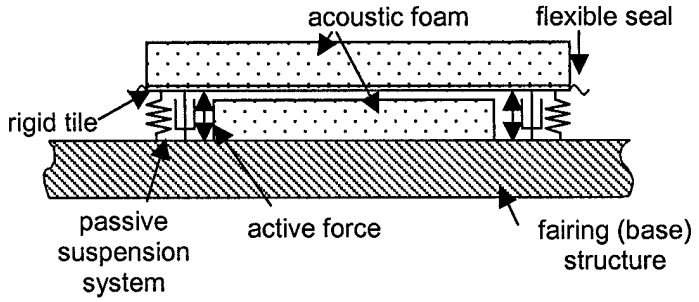

Figure 13. Smart active-passive tile arrangement.

As the tiles are very stiff they do not have flexible response and only have rigid body motion at low frequencies (well below their fundamental bending resonance). The rigid body motions are shown in Figure 14.

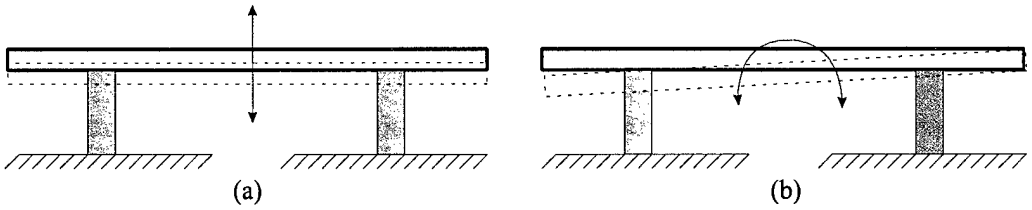

Figure 14. System rigid body modes (a) heave, (b) pitch.

Since the tiles are rigid then they radiate sound like individual pistons and the sound transmitted to the fairing interior is directly proportional to the tile normal displacement. Reducing the tiles normal displacement will thus result in a drop of transmitted sound power to the fairing interior.

The arrangement is a variation of a classic vibration isolation problem [5]. Above the resonance of the tile-spring/damper system, normal vibrations of the base structure (the payload fairing) will be poorly transmitted to the tile resulting in a drop of transmitted sound. The passive dynamics of the tile suspension system thus should result in passive attenuation. In addition acoustic foam is located under and above the tile to increase the high frequency passive transmission loss. However at the resonance of the tile suspension system, the tile normal motion is large resulting in an *increase* in transmitted sound. We compensate for this increase by locating active forces in parallel with the mounts to actively reduce the tile normal motion (and thus transmitted sound) near the tile resonance. In addition we design the dynamics so that the tile resonance is at low frequency where passive attenuations are poor.

Such an arrangement also leads to a very simple active control approach consisting of simple feedback loops closed around each mount as shown in Figure 14. The feedback control system can be analog and uncoupled since bending response of the tile is negligible. The control objective would be to reduce the tile motion at feedback accelerometer sensors, which are located above each mount on the tile. Analysis has demonstrated that such a control strategy of using suppression of the heave mode of the tile but not the rocking mode leads to good reduction of radiated sound [6]. Figure 15 shows the radiation efficiency of a baffled simply supported beam covered with either five or ten active tiles. The results show that the radiation efficiency of the third beam mode (for example) is significantly reduced below the coincidence frequency and that rocking motion only becomes significant when the acoustic wavelength is similar to the tile transverse size.

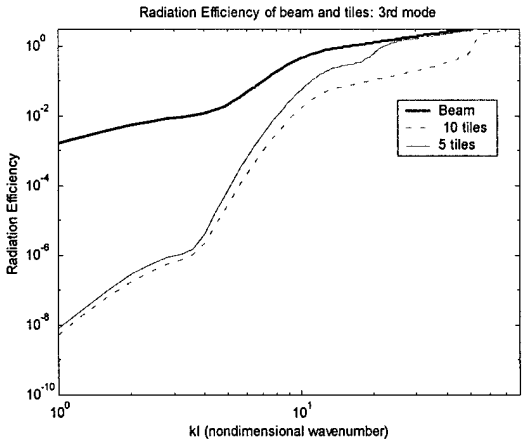

Figure 15. Radiation efficiency of a simply supported beam vibrating in its 3rd mode and covered with 5 or 10 tiles. Active control is applied to cancel the heave motion only.

A couple of aspects of the arrangement should be considered. The use of isolators connecting the tiles to the base structure (the payload fairing) results in good passive isolation above the resonance of the tile-suspension system. However the tile is also coupled to the normal motion of the fairing by the sound field in the cavity under the tile. At very low frequencies, below the fundamental cavity resonance, this air mass is very stiff and motion of the fairing will be directly transmitted to the tile resulting in poor passive attenuation. There are two solutions to this problem. Firstly the acoustic space can be filled with foam in order to reduce the acoustic response. Secondly the active forces in parallel with the mounts can compensate for the sound transmission. Other important aspects are that the complete active-passive smart blanket should be compact and of the order of the size of conventional treatments. Obviously the treatment should not be too heavy-we set a target weight of the treatment to be a maximum of 10% of the base structure. The active system should also be compact and of low complexity. Here the SISO analog feedback loops are promising since all the sensors and control electronics can be integrated into the smart blanket close to each mount.

In order to demonstrate the potential of the approach in this report we analytically and experimentally investigate the performance of a single active tile designed to perform hybrid active/passive attenuation of sound transmitted through a vibrating panel. The report first considers the construction of the active tile including compact active mounts. Tests are then performed with the active tiles. The results are then extrapolated to real application sound levels to investigate whether the proposed active tile has sufficient control authority for a realistic payload fairing application.

3.3 Construction of the Active Tile

There are two main design aspects of the active tile: the tile material itself and the active mounts. To achieve a very light surface treatment, which is very stiff at low frequencies, it is necessary to carefully choose the tile material properties and construction. In the work reported here we used a carbon/fiber Nomex honeycomb composite sandwich material of 6 cm thickness and of 1.0 kg weight per unit area. The size of the tile for these tests was chosen to be 30 cm by 38 cm. The first bending resonance of the free panel was estimated to be 330 Hz, which is well out of the frequency range of interest.

The second important aspect was to design and implement the active-passive isolation mounts. As stated before it is necessary that the active mounts have a passive spring isolation arrangement with active forces in parallel. The active mounts have to be compact and should have enough control authority for the real application. For this application we chose to use THUNDER elements as the active actuators. The THUNDER actuator is composed of three thin layers of a steel base layer, a piezoceramic patch and an aluminum top cover sheet bonded together under temperature. On cooling, due to differential thermal expansion, the THUNDER element consists of a curved unimorph transducer as shown in Figure 16. Due to the unimorph and curved nature of the THUNDER element, when a voltage is applied, the element will deform and generate a force in the direction normal to its curvature as shown in Figure 16.

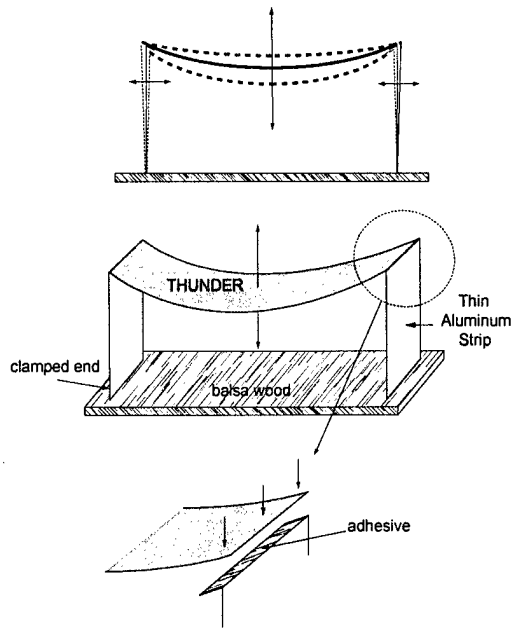

Figure 16. Active-passive isolation mount using a THUNDER piezoelectric element.

In the current active tile application the THUNDER element is glued along its straight edges to very thin aluminum strips whose bottom edges are attached to thin balsa wood base as illustrated in Figure 16. The complete arrangement is then connected between the tile and the base structure as shown in Figure 17.

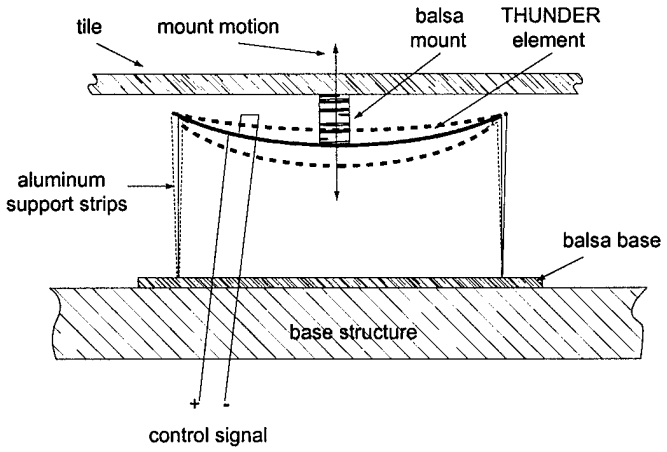

Figure 17. Schematic of installation of active-passive isolation mount with tile.

This arrangement allows for the tile to be elastically suspended by the natural stiffness of the THUNDER elements and attached thin aluminum side strips. In addition, applying a voltage to the element will allow the active mount to apply active forces in between the tile and the base structure at each mount point as shown in Figure 17. Figure 18 shows a picture of a single active mount mounted to a Nomex tile used in the tests to be discussed next.

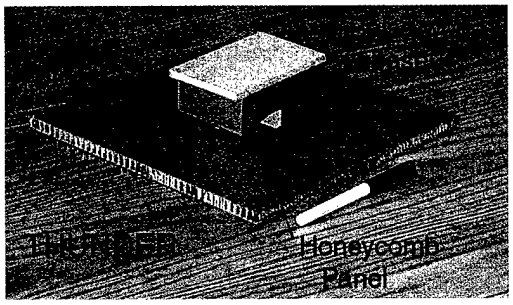

Figure 18. Active tile used for SDOF isolation tests.

3.4 Experimental Tests

Example results of a preliminary experimental investigation of the performance of the approach are now presented. Two main tests were performed. Firstly the active tile was directly mounted on top of a large shaker to directly measure its passive and active vibration isolation performance for a single actuator/ SDOF arrangement. Secondly, an acoustic transmission loss experiment using a single tile suspended by two active mounts and positioned on an aluminum panel was carried out. For both of these tests the active tile was investigated without being embedded in acoustic foam. Future tests will include acoustic foam on top of the tile surface and in the acoustic cavity under the tile.

3.5 Vibration isolation tests

The first experimental set of tests investigated the passive and active vibration isolation characteristics of a single active tile. A smart tile of dimensions 25 cm by 25m was located on top of a 25 lb electrodynamic vibration shaker as shown in Figure 19. The arrangement simulates a point SDOF excitation of the active tile system. The test set up is of reduced complexity since it does not take into account effects such as mechanical coupling of adjacent tiles, acoustic radiation and gaps between adjacent tiles. However it does allow the investigation of the passive and active isolation performance of the THUNDER active mount.

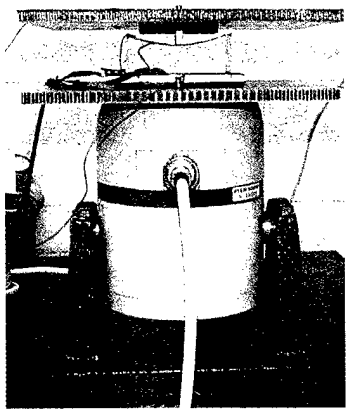

Figure 19. Experimental setup for isolation tests.

The shaker was driven with band-limited white noise from 0 to 250Hz. The normal acceleration of the shaker drive point and the tile were measured to compute the transmissibility (inverse of vibration isolation) of the tile-mount system. The active control approach used for these tests was the feedfoward LMS algorithm [5]. Used to minimize the signal from the accelerometer located on the tile.

Figure 20 shows the acceleration response of the shaker drive point and the active tile with and without active control applied. A resonance of the suspension system is observed near 20 Hz. Above the resonance the tile suspension system provides good passive reduction of transmitted vibration. At the resonance the transmitted vibration is passively amplified as expected. When the active control is turned on the vibration amplification at resonance is eliminated and active-passive attenuations of transmitted vibrations of the order of 20dB over the design bandwidth of 0 to 250 Hz are observed.

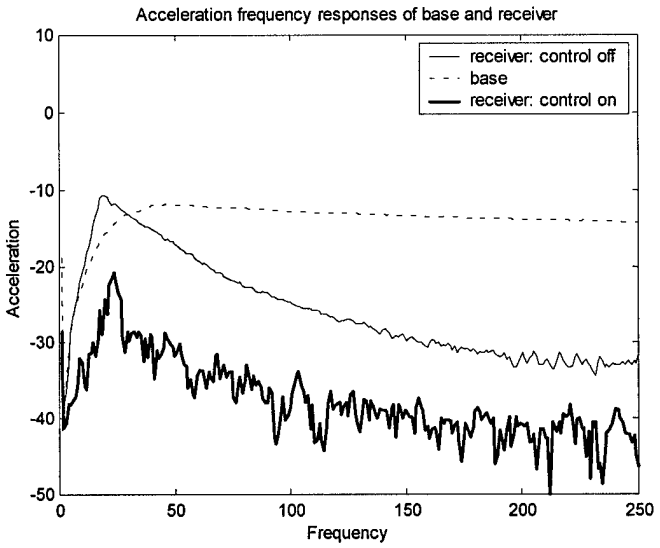

Figure 20. Experimentally measured base and tile acceleration without (passive) and with active control (active-passive).

The transmissibility of the system calculated from these results is presented in Figure 21 with and without active control. Very good vibration control is observed for the active-passive tile system.

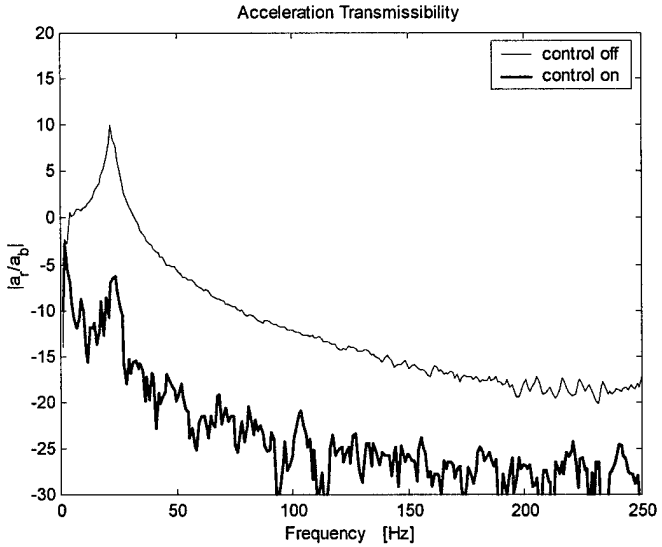

Figure 21. Experimentally measured transmissibility of active tile, without control (faint line) and with control (bold line).

These initial tests confirm the potential of the active-passive tile isolation approach. If the interior surface of the fairing could be coated with a skin of such tiles then the transmitted sound would be significantly

reduced over a wide band of low frequencies since it is directly coupled tot he vibration. We now evaluate the acoustic transmission characteristics of the active tile.

3.6 Acoustic transmission loss tests

In these set of tests the use of the active tile to control transmission of sound through a test panel was investigated. In this case a Nomex panel of size 30 cm by 38 cm in conjunction with two active THUNDER mounts was used. The test tile is shown in Figure 22.

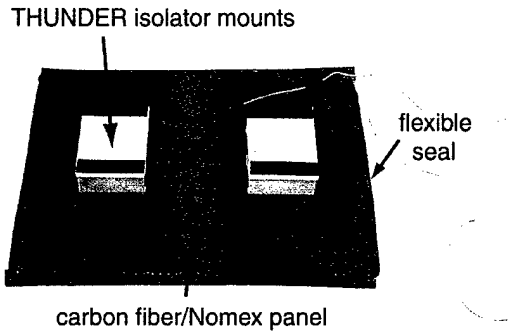

Figure 22. Active tile prototype for sound transmission control tests.

A schematic of the experimental test set up is shown in Figure 23. In these tests a 1.6 mm thick, 30cm by 38 cm aluminum panel was clamped in the test hole of the VAL transmission loss test facility. The single tile shown in Figure 22 was located on the aluminum baseline test plate. The gaps at the edge of the panel were sealed with a flexible foam gasket. A loudspeaker located inside the reverberant source room was used to excite the panel with broadband noise. The transmitted sound level was measured in the anechoic receiving chamber of the transmission loss test facility using 9 microphones located on a hemispherical array surrounding the plate. The microphones were in the far field of the plate radiation. The active control paradigm for these tests was again the feedforward LMS algorithm used to actively minimize the tile acceleration at two points above each mount location by driving the two THUNDER active mounts with independent control signals. Figure 24 shows a picture of the active tile mounted on the base panel.

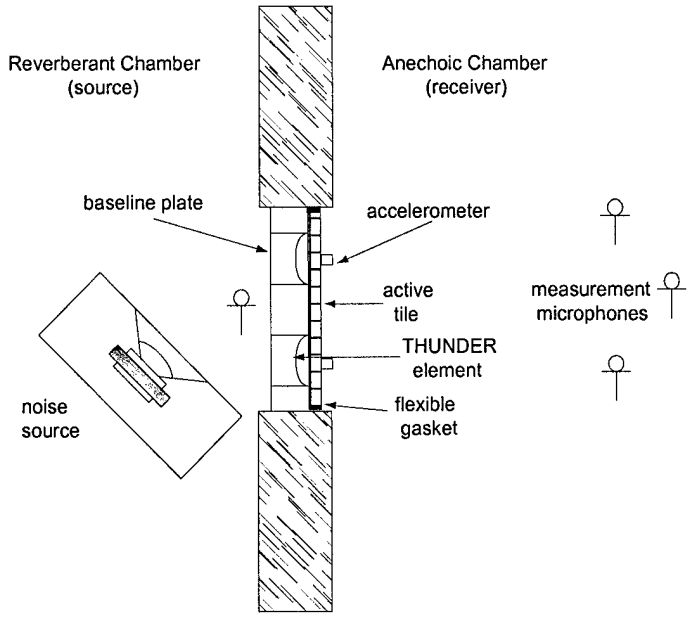

Figure 23. Schematic of test arrangement for sound transmission control.

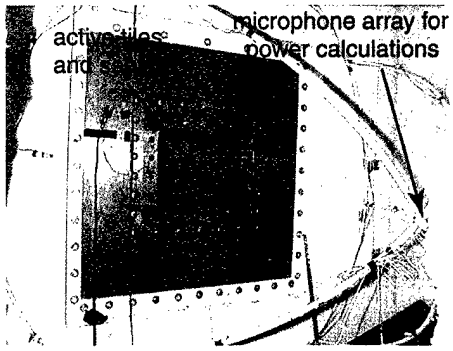

Figure 24. Photograph of active tile mounted on base plate in wall of transmission loss test facility. Note also microphone hemisphere for estimating radiated sound power.

Figure 25 presents the relative acceleration of the baseline plate structure and the acceleration of the active tile without control (passive case) and with control (active case). Note that the panel-suspension system exhibits a resonance near 120Hz. and provides good passive attenuation of transmitted vibration above the resonance. The application of the control leads to significant reductions near the panel resonance and even at higher frequencies.

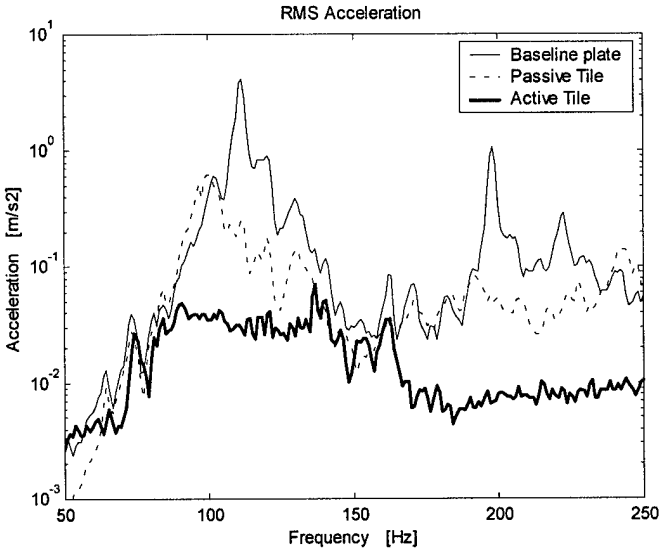

Figure 25. Acceleration of base plate and active tile without and with control.

We now turn to the transmitted acoustic field. Figure 26 presents the measured sound power transmitted into the anechoic receiving chamber (the transmitted field) calculated from the microphones on the hemispherical array for the various test cases. The results again show high active-passive reductions of the transmitted sound levels over the complete test frequency band. Finally Figure 27 presents the transmission loss of the baseline panel with the active tile in place calculated from the ratio of the transmitted pressures to the incident acoustic pressure in the source room. Again it is evident that the active tile leads to large increases in transmission loss over many parts of the bandwidth and, most significantly, always increases the magnitudes of the low transmission loss regions of the bare panel. Note that the attenuations are less than that shown by the panel vibrations and this is most likely due to acoustic leakage through the seals at the edges of the tile.

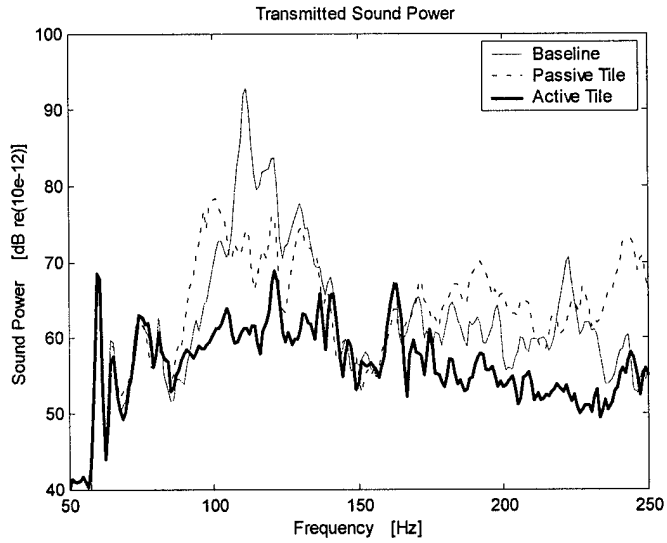

Figure 26. Transmitted power of base plate, base plate covered with active tile, no control (passive) and base plate covered with active tile, control on (active-passive).

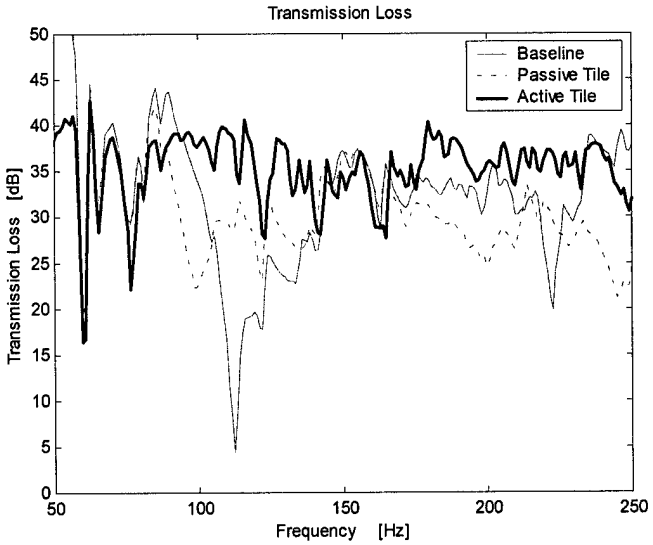

Figure 27. Calculated transmission losses corresponding the tests of Figure 26.

3.7 Theoretical Analysis

In this section we describe preliminary work to model the active tile system. The theoretical model consists of a clamped aluminum plate mounted in an infinite baffle. A very stiff plate with free boundary conditions is connected to the base plate by spring –damper isolators systems. Active forces are located in parallel to the isolator (mounts). The base panel is excited by an incident plane wave and the tile radiates into free space. The stiff plate is assumed to be acoustically sealed at the edges. The system is shown schematically in Figure 28. The model should allow further investigation and parameter optimization of the active tile approach on validation with the experimental results.

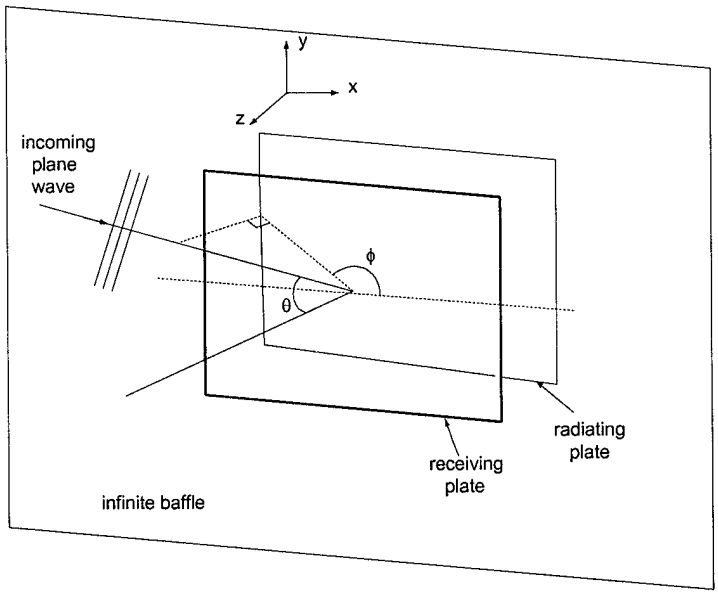

Figure 28. Double panel and incident acoustic wave coordinate systems for analytical model.

In order to develop the model, it is necessary to derive the general equations of motion of a double panel system coupled by the isolators and driven by an acoustic field. The isolators are approximated point spring/dampers connecting both plates with a parallel active force. The dynamics of the contained acoustic field between the base structure and the tile is modeled using the rigid walled cavity modes.

The equations of motion of the incident (subscript 1) and radiating (subscript 2) plates connected by a set of spring-dampers can be written as:

$$D_1\nabla^4 w_1 + m_1\frac{\partial^2 w_1}{\partial t^2} + c(\frac{\partial w_1}{\partial t} - \frac{\partial w_2}{\partial t})\sum_{j=1}^{J}\sum_{i=1}^{I}\delta(x-x_j)\delta(y-y_i)$$
$$+ k(w_1 - w_2)\sum_{j=1}^{J}\sum_{i=1}^{I}\delta(x-x_j)\delta(y-y_i) = f_e - p(x,y,0) \quad (1)$$

$$D_2\nabla^4 w_2 + m_2\frac{\partial^2 w_2}{\partial t^2} + c(\frac{\partial w_2}{\partial t} - \frac{\partial w_1}{\partial t})\sum_{j=1}^{J}\sum_{i=1}^{I}\delta(x-x_j)\delta(y-y_i)$$
$$+ k(w_2 - w_1)\sum_{j=1}^{J}\sum_{i=1}^{I}\delta(x-x_j)\delta(y-y_i) = p(x,y,L_z) + f_c \quad (2)$$

Where:

w_1 and w_2 are the normal displacements of plates 1 and 2
D_1 and D_2 are the bending stiffness of plates 1 and 2
c is the damping coefficient of the isolators
k is the stiffness of the isolators
x_i and y_j are the isolators' coordinates
f_e is the external disturbance
f_c are the control forces
p is the pressure field between the plates

The sound field in the cavity between the two plates can be written in terms of the velocity potential of the acoustic field as:

$$\Lambda_n(\omega_n^2 - \omega^2)a_n = -c^2\sum_{n}^{N} C_{nm}\dot{q}_m \quad (3)$$

Where a_n are the coefficients of the velocity potential expanded in terms of the acoustic modes of the cavity Ψ_n:

$$\varphi = \sum_{n=1}^{N} a_n\Psi_n$$

and Λ_n is the nth acoustic modal mass.

The acoustic velocity potential is related to the pressure by Bernoulli's equation:

$$p = -\rho\dot{\varphi}$$

Assuming that both plates have the same modes shapes Φ_m and expressing the plate displacements as a modal expansion, one can substitute this modal expansion back into the equations above. Making use of the orthogonality conditions and the Dirac delta sifting properties to get:

$$M_{1mp}[\omega^2 + (i\omega c + k)X_{nm}(x_j, y_i) - \omega_{1m}^2]q_{1m} - [(i\omega c + k)X_{nm}]q_{2m} = F_e - P(x, y, 0) \quad (4)$$

$$M_{2mp}[\omega^2 + (i\omega c + k)X_{nm}(x_j, y_i) - \omega_{2m}^2]q_{2m} - [(i\omega c + k)X_{nm}]q_{1m} = F_c + P(x, y, L_z) \quad (5)$$

Where:

$$F_e = \int_S \Phi_m f_e ds$$

$$F_c = \int_S \Phi_m f_c ds$$

$$P = -\rho \sum_n^M \dot{a}_n C_{nm}(x, y, z)$$

$$X_{nm} = \sum_{j=1}^{J} \sum_{i=1}^{I} \sum_{m=1}^{M} \sum_{n=1}^{N} \Phi_m(x_j, y_i)\Phi_n(x_j, y_i)$$

Using the above analysis we can predict the sound transmitted through the base plate, the base plate covered with a passive tile and the base plate covered with an active tile. At this stage we have not included the control analysis so we limit our results to the passive configurations. Figure 29 shows the predicted sound power transmitted through a single aluminum clamped panel of the same thickness as the experiment discussed above. The panel is excited by an acoustic plane wave incident at 45 deg as in the experiment. Good agreement between theory and experiment is evident with the model accurately predicting the system resonances and radiated power levels across the 50-250 Hz design bandwidth. High sound power transmission is evident at the resonance frequency of the base structure fundamental mode near 120Hz.

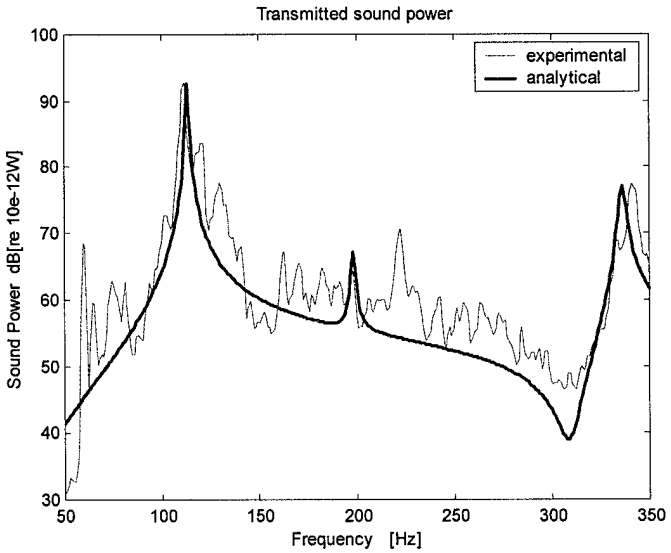

Figure 29. Predicted versus measured power transmitted through a clamped aluminum plate in a baffle.

Figure 30 now shows theoretical and experimental results when the active-passive tile is located on the base panel. In this case there is no control, so the effects are entirely due to the passive isolator dynamics of

the tile and its suspension system. Good agreement between theory and experiment is again evident below 200Hz. At higher frequencies the results diverge somewhat and this is most likely due to; (1) sound transmitted through the edge gaps of the tile, (2) a flexible mode of the THUNDER mount at 330Hz and (3) rocking motion of the tile (considered to be only normal motion in the model).

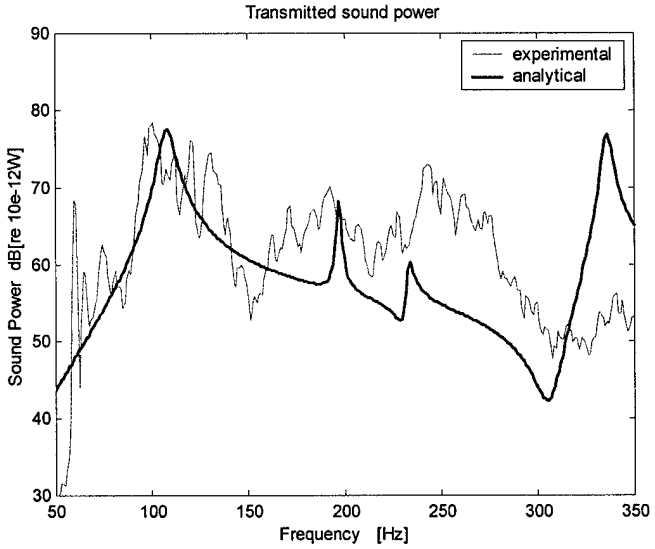

Figure 30. Predicted versus measured power transmitted through a double panel system consisting of a clamped plate covered by a active tile isolation system (no control).

Comparing Figures 29 and 30 it is evident that the tile system leads to good passive isolation of the transmitted sound below 250Hz particularly at the base panel fundamental resonances. There is some increase in transmitted sound power at higher frequencies but this likely to be controlled by the later insertion of the acoustic foam elements. Application of active control will also lead to improved reduction in radiated sound power across the complete design bandwidth.

3.8 Practical Aspects of the Use of Active Tiles in a Real Payload Fairing Application

The preliminary tests summarized above have demonstrated the potential for the active tiles for controlling sound transmitted into payload fairing structures. In order for such an approach be of practical use in the real application, various implementation and performance parameters need to be estimated

3.9 Weight and thickness of the treatment

Since the active skin approach employed here works by decoupling the sound field from the vibrating fairing it is necessary to cover all of the inside fairing surface or a major part of it. For the active tile configuration considered here an added weight estimate can be calculated as: the carbon fiber/Nomex tile was 6mm thick and has a surface density of 1.0 kg/m^2. The THUNDER active mounts each weighed 20 grams. Two independent analog feedback control and power circuits would be needed at a weight of 8 grams each. Considering a launch vehicle payload fairing that has a typical surface density of 9.0 kg/m^2, the added weight of the treatment is calculated to be approximately 14 %. This value is slightly larger than the target 5-10% added treatment weight but should be realizable by optimizing the tile material and active mounts. Note that the acoustic foam is not included in the calculation on the assumption that the active tile will be embedded in the existing foam treatment.

The active tile treatment proposed here is of 5cm thickness, which compares well with the 7.5cm thickness of present acoustic foam treatments in fairings.

3.10Maximum controllable sound levels with the active tile

Another very important aspect is the maximum sound level that the active tile can control. This value will be limited by the maximum voltage that can be applied across the THUNDER piezoelectric elements. We base the estimates on the results of the acoustic transmission loss tests of the active tile. These experiments were performed with an incident acoustic wave of total sound pressure level of 128dB over a 50- 250Hz bandwidth. For this level of incident excitation it was necessary to apply around 80 V rms to each active mount in order to reduce the transmitted sound. Since the maximum applicable voltage to the THUNDER elements is around 215 V rms, it is possible to calculate by extrapolation that the maximum incident sound pressure that could be controlled is approximately 137dB. This value is close to that of typical launch vehicle excitation loads [1]. Note however, that this result is dependent on the base structure dynamics, which in this case is an aluminum panel not a real fairing.

We thus also estimate the maximum controllable vibration levels and see how they compare to the vibration of an actual fairing structure. For the experiments discussed above the base panel vibration was measured to be 2.7g rms over the 0 to 200 Hz bandwidth without the tile treatment in place. Locating the active-passive tile treatment leads to both passive attenuation and further active reduction of the vibration when the control is turned on. The required control voltage is again 80 V rms. Using extrapolation to the maximum allowable voltage we can calculate that the active-passive tile will be able to control vibrations of the untreated base structure 7.2 g rms. This compares well with typical observed normal vibration levels of real fairings of approximately 7.5 g rms [7].

3.11Conclusion

An experimental and preliminary analytical investigation of the use of smart acoustic tiles to control sound transmission into fairing like structures has been carried out. The experiments have demonstrated the high potential of the active tile approach to reduce realistic payload noise in a relatively lightweight, conformal installation. The analytical model has demonstrated good agreement between predictions and experiments and will be useful for efficient investigations of system parameter changes, system configuration improvements and optimal design. Embedding the active tiles into acoustic foam will allow the final development of a "smart acoustic blanket".

3.12Future Work

The above investigations have demonstrated the potential of the smart tile approach. However there remains much work to be carried out to develop, implement and test necessary components. These are;

- Embed the active tile in acoustic foam and test.
- Develop analog SISO feedback controllers, implement and test.
- Investigate and improve performance limitation due to tile edge air gaps
- Apply multiple tiles to a panel section of a Delta V fairing in TL facility.
- Test multiple tiles on selected panel radiating into a rigid enclosure.
- Extend model to include both SISO feedback and MIMO feedforward control.
- Extend the model to multiple tiles.
- Optimal design tile treatment.
- Apply tile treatment to a real payload fairing or full-scale cylinder model of fairing.

3.13References

1. Bradford, L. and Manning, J.E., "Attenuation of the Cassini Spacecraft Acoustic Environment", Sound and Vibration, October, pp.30-37, 1996.
2. Fuller, C.R., Rogers, C.A. and Liang, C. "Active Foam for Noise and Vibration Control, U.S. Patent No. 5,719,945,1998.
3. Gentry, C.A., Guigou, C. and Fuller, C.R., "Smart Foam for Applications in Passive/Active Noise Radiation Control", Journal of the Acoustical Society of America, Vol. 101(4), pp. 1771-1778, 1999.
4. Fuller, C. R, Guigou, C. and Johnson, B.D. "Control of Sound Radiated from Structures Using Active Skins', Proceedings of Ibero-American Congress of Acoustics, 18th SOBRAC Meeting, Santa Catarina, Brazil, Vol. 1, pp.186-197, 1998.
5. Fuller, C.R., Elliott, S.J and Nelson, P.A., "Active Control of Vibration", Academic Press, London, 1996.
6. Johnson, M.E. and Elliott, S.J., "Active Control of Sound Radiation From Vibrating Surfaces Using Arrays of Discrete Actuators " Journal of Sound and Vibration, Vol. 207(5), pp.743-759, 1997.
7. Osman, H., "Personal Communication", Boeing Space and Communications, Huntington Beach, CA, 2000.

5. PERSONNEL SUPPORTED

Andre Goldstein, Ph.D. Graduate Student
Dr. Mike Kidner, Research Associate
Dr. Chris Fuller, Professor and project PI

6. PUBLICATIONS

Fuller, C. R., "Active-Passive Control of Sound with Smart Skins," *Keynote Address* to the 8th AIAA/CEAS Aeroacoustics Conference and Exhibit, Breckenridge, CO, June 17-19, 2002.

Fuller, C. R., "Active Control of Sound Radiation from Structures: Progress and Future Directions," *Plenary Lecture* to ACTIVE 2002, p. 3-28, Southampton, UK, July 15-17, 2002.

Goldstein, A. and Fuller, C. R., "Control of Sound Transmission with Active-Passive Tiles," Proceedings of ACTIVE 2002, pp. 547-558, Southampton, UK, July 15-17, 2002.

C. R. Fuller, "Active Control: Feedforward Control of Vibration," Volume 2, pp. 513-520, The Encyclopedia of Vibration, S. G. Braun, D. J. Ewins and S. S. Rao, Editor, Academic Press, September, 2001.

Fuller, C. R., "Smart Skins for Sound Control," Volume 2, pp. 1029-1037, The Encyclopedia of Smart Materials, John Wiley and Sons, Inc., October, 2001.

7. INTERACTIONS/TRANSITIONS

(a) Participations at meetings:

Fuller, C. R., "Active-Passive Control of Sound with Smart Skins," *Keynote Address* to the 8th AIAA/CEAS Aeroacoustics Conference and Exhibit, Breckenridge, CO, June 17-19, 2002.

Fuller, C. R., "Active Control of Sound Radiation from Structures: Progress and Future Directions," *Plenary Lecture* to ACTIVE 2002, p. 3-28, Southampton, UK, July 15-17, 2002.

Goldstein, A. and Fuller, C. R., "Control of Sound Transmission with Active-Passive Tiles," Proceedings of ACTIVE 2002, pp. 547-558, Southampton, UK, July 15-17, 2002.

Fuller, C. R., "Control of Sound Radiation and Reflection with Advanced Smart Acoustic Blankets," presented at the *AFOSR Contractor's Meeting in Mechanics of Composite Materials and Structural Mechanics*, Arlington, VA, September 25-27, 2002.

Fuller, C. R., "Control of Sound Radiation and Reflection with Advanced Smart Acoustic Blankets," presented at the *AFOSR Contractor's Meeting in Mechanics of Composite Materials and Structural Mechanics*, Arlington, VA, October 18-20, 2001.

(b) *Consultative/advisory functions.* None

(c) *Transitions:* Throughout the past year there has been a strong coordination with Phillips Laboratories at Kirtland Air Force Base (POC: Dr. Steve Lane) and Boeing Space and Communications, Delta IV program (POC: Dr. Haisam Osman). This has involved regularly establishing AF and industry needs for the launch vehicle noise control application and transmitting of the research program results. Future cooperation on a sounding rocket flight test of the technology has been discussed with the AF. Future cooperation with Boeing S&C will involve testing the smart tile approach on the Boeing composite payload cylinder.

8. NEW DISCOVERIES

None

9. HONORS/AWARDS

The 2000 Dean's Award for Excellence in Research, April 4, 2000.